galaxies

MDPI

Article

Padé Approximant and Minimax Rational Approximation in Standard Cosmology

Lorenzo Zaninetti

Dipartimento di Fisica, Università degli Studi di Torino, via P.Giuria 1, I-10125 Turin, Italy; zaninetti@ph.unito.it

Academic Editor: Emilio Elizalde
Received: 12 November 2015/ Accepted: 21 January 2016/ Published: 18 February 2016

Abstract: The luminosity distance in the standard cosmology as given by ΛCDM and, consequently, the distance modulus for supernovae can be defined by the Padé approximant. A comparison with a known analytical solution shows that the Padé approximant for the luminosity distance has an error of 4% at redshift = 10. A similar procedure for the Taylor expansion of the luminosity distance gives an error of 4% at redshift = 0.7; this means that for the luminosity distance, the Padé approximation is superior to the Taylor series. The availability of an analytical expression for the distance modulus allows applying the Levenberg–Marquardt method to derive the fundamental parameters from the available compilations for supernovae. A new luminosity function for galaxies derived from the truncated gamma probability density function models the observed luminosity function for galaxies when the observed range in absolute magnitude is modeled by the Padé approximant. A comparison of ΛCDM with other cosmologies is done adopting a statistical point of view.

Keywords: cosmology; observational cosmology; distances; redshifts; radial velocities; spatial distribution of galaxies; magnitudes and colors; luminosities

PACS: 98.80.-k; 98.80.Es; 98.62.Py; 98.62.Qz

1. Introduction

In order to obtain astronomical observables, such as the distance modulus and the absolute magnitude for supernovae (SN) of Type Ia in the standard cosmological approach, as given by the ΛCDM model, we need the evaluation of the luminosity distance, which is derived from the comoving distance. At the moment of writing, there is no analytical expression for the integral of the comoving distance in ΛCDM, and a numerical integration should be implemented. An analytical expression for the integral of the comoving distance in ΛCDM can be obtained by adopting the technique of the Padé approximant; see [1–3]. Once an approximate solution is obtained for the luminosity distance, we can evaluate the distance modulus and the absolute magnitude for SNs. Furthermore, the minimax rational approximation can provide a compact formula for the two above astronomical observables as functions of the redshift. From an observational point of view, the progressive increase in the number of supernova (SN) of Type Ia for which the distance modulus is available, 34 SNein the sample, which produced evidence for the accelerating universe (see [4]), 580 SNe in the Union 2.1 compilation (see [5]) and 740 SNe in the joint light-curve analysis (JLA) (see [6]), allows analyzing both the ΛCDM and other cosmologies from a statistical point of view. The statistical approach to cosmology is not new and has been recently adopted by [7,8]. In order to cover the previous arguments, Section 2 introduces the Padé approximant and determines the basic integral of the ΛCDM, which allows deriving the approximate luminosity distance. The approximate magnitude here derived is applied to parametrize a new luminosity function for galaxies at high redshift; see Section 3. The distance modulus in different

cosmologies is reviewed, and the main statistical parameters connected with the distance modulus are derived; see Section 4.

2. The Standard Cosmology

This section introduces the Hubble distance, the dark energy density, the curvature, the matter density and the comoving distance (which is presented as the integral of the inverse of the Hubble function). In the absence of a general analytical formula for the comoving distance, we introduce the Padé approximation. As a consequence, we deduce an approximate solution for the transverse comoving distance, the luminosity distance and the distance modulus. The shift that the Padé approximation introduces in the relationship for the poles is discussed. The calibration of the Padé approximation for the distance modulus on two astronomical catalogs allows deducing the minimax polynomial approximation for the observed distance modulus for SNs of Type Ia.

2.1. The Padé Approximant

We use the same symbols as in [9], where the Hubble distance D_{H} is defined as:

$$D_{\mathrm{H}} \equiv \frac{c}{H_0} \tag{1}$$

We then introduce the first parameter: Ω_{M}

$$\Omega_{\mathrm{M}} = \frac{8\pi\, G\, \rho_0}{3\, H_0^2} \tag{2}$$

where G is the Newtonian gravitational constant and ρ_0 is the mass density at the present time. The second parameter is Ω_Λ:

$$\Omega_\Lambda \equiv \frac{\Lambda\, c^2}{3\, H_0^2} \tag{3}$$

where Λ is the cosmological constant; see [10]. The two previous parameters are connected with the curvature Ω_K by:

$$\Omega_{\mathrm{M}} + \Omega_\Lambda + \Omega_K = 1 \tag{4}$$

The comoving distance, D_{C}, is:

$$D_{\mathrm{C}} = D_{\mathrm{H}} \int_0^z \frac{dz'}{E(z')} \tag{5}$$

where $E(z)$ is the 'Hubble function':

$$E(z) = \sqrt{\Omega_{\mathrm{M}}\,(1+z)^3 + \Omega_K\,(1+z)^2 + \Omega_\Lambda} \tag{6}$$

The above integral does not have an analytical formula, except for the case of $\Omega_\Lambda = 0$, but the Padé approximant (see Appendix B) gives an approximate evaluation, and the indefinite integral is (B3), where the coefficients a_j and b_j can be found in Appendix A. The approximate definite integral for (5) is therefore:

$$D_{\mathrm{C},2,2} = F_{2,2}(z; a_0, a_1, a_2, b_0, b_1, b_2) - F_{2,2}(0; a_0, a_1, a_2, b_0, b_1, b_2) \tag{7}$$

The transverse comoving distance D_{M} is:

$$D_{\mathrm{M}} = \begin{cases} D_{\mathrm{H}} \dfrac{1}{\sqrt{\Omega_K}} \sinh\left[\sqrt{\Omega_K}\, D_{\mathrm{C}}/D_{\mathrm{H}}\right] & \text{for } \Omega_K > 0 \\ D_{\mathrm{C}} & \text{for } \Omega_K = 0 \\ D_{\mathrm{H}} \dfrac{1}{\sqrt{|\Omega_K|}} \sin\left[\sqrt{|\Omega_K|}\, D_{\mathrm{C}}/D_{\mathrm{H}}\right] & \text{for } \Omega_K < 0 \end{cases} \tag{8}$$

and the approximate transverse comoving distance $D_{\mathrm{M},2,2}$ computed with the Padé approximant is:

$$D_{\mathrm{M},2,2} = \begin{cases} D_{\mathrm{H}} \dfrac{1}{\sqrt{\Omega_K}} \sinh\left[\sqrt{\Omega_K}\, D_{\mathrm{C},2,2}/D_{\mathrm{H}}\right] & \text{for } \Omega_K > 0 \\ D_{\mathrm{C},2,2} & \text{for } \Omega_K = 0 \\ D_{\mathrm{H}} \dfrac{1}{\sqrt{|\Omega_K|}} \sin\left[\sqrt{|\Omega_K|}\, D_{\mathrm{C},2,2}/D_{\mathrm{H}}\right] & \text{for } \Omega_K < 0 \end{cases} \tag{9}$$

An analytic expression for D_{M} can be obtained when: $\Omega_\Lambda = 0$:

$$D_{\mathrm{M}} = D_{\mathrm{H}} \frac{2\left[2 - \Omega_{\mathrm{M}}\,(1-z) - (2-\Omega_{\mathrm{M}})\sqrt{1+\Omega_{\mathrm{M}}\, z}\right]}{\Omega_{\mathrm{M}}^2\,(1+z)} \text{ for } \Omega_\Lambda = 0 \tag{10}$$

This expression is useful for calibrating the numerical codes, which evaluate D_{M} when $\Omega_\Lambda \neq 0$.
The luminosity distance is:

$$D_{\mathrm{L}} = (1+z)\, D_{\mathrm{M}} \tag{11}$$

which in the case of $\Omega_\Lambda = 0$ becomes:

$$D_{\mathrm{L}} = 2\,\frac{c\left(2 - \Omega_M\ (1-z) - (2-\Omega_M)\sqrt{z\Omega_M + 1}\right)}{H_0 {\Omega_M}^2} \tag{12}$$

and the distance modulus when $\Omega_\Lambda = 0$ is:

$$m - M = 25 + 5\,\frac{1}{\ln(10)} \ln\!\left(2\,\frac{c\left(2 - \Omega_M\,(1-z) - (2-\Omega_M)\sqrt{z\Omega_M+1}\right)}{H_0 {\Omega_M}^2}\right) \tag{13}$$

The Padé approximant luminosity distance when $\Omega_\Lambda \neq 0$ is:

$$D_{\mathrm{L},2,2} = (1+z)\, D_{\mathrm{M},2,2} \tag{14}$$

and the Padé approximant distance modulus, $(m-M)_{2,2}$, in its compact version, is:

$$(m-M)_{2,2} = 25 + 5\log_{10}(D_{\mathrm{L},2,2}) \tag{15}$$

and, as a consequence, the Padé approximant absolute magnitude, $M_{2,2}$, is:

$$M_{2,2} = m - 25 - 5\log_{10}(D_{\mathrm{L},2,2}) \tag{16}$$

The expanded version of the Padé approximant distance modulus is:

$$(m-M)_{2,2} = 25 + 5\,\frac{1}{\ln(10)} \ln\left(\frac{c\,(1+z)}{H_0\sqrt{\Omega_K}} \sinh\left(1/2\,\frac{\sqrt{\Omega_K}A}{{b_2}^2\sqrt{4\,b_0 b_2 - {b_1}^2}}\right)\right) \tag{17}$$

with:

$$\begin{aligned} A \;=\; & \ln\left(z^2 b_2 + z b_1 + b_0\right) a_1 b_2 \sqrt{4\,b_0 b_2 - {b_1}^2} - \ln\left(z^2 b_2 + z b_1 + b_0\right) a_2 b_1 \sqrt{4\,b_0 b_2 - {b_1}^2} \\ & - \ln(b_0)\, a_1 b_2 \sqrt{4\,b_0 b_2 - {b_1}^2} + \ln(b_0)\, a_2 b_1 \sqrt{4\,b_0 b_2 - {b_1}^2} + 2\,a_2 z b_2 \sqrt{4\,b_0 b_2 - {b_1}^2} \\ & + 4\,\arctan\left(\frac{2\,z b_2 + b_1}{\sqrt{4\,b_0 b_2 - {b_1}^2}}\right) a_0 {b_2}^2 - 2\,\arctan\left(\frac{2\,z b_2 + b_1}{\sqrt{4\,b_0 b_2 - {b_1}^2}}\right) b_1 a_1 b_2 \end{aligned}$$

$$-4\ \arctan\left(\frac{2\,z b_2 + b_1}{\sqrt{4\,b_0 b_2 - {b_1}^2}}\right) a_2 b_0 b_2 + 2\ \arctan\left(\frac{2\,z b_2 + b_1}{\sqrt{4\,b_0 b_2 - {b_1}^2}}\right) {b_1}^2 a_2$$
$$-4\ \arctan\left(\frac{b_1}{\sqrt{4\,b_0 b_2 - {b_1}^2}}\right) a_0 {b_2}^2 + 2\ \arctan\left(\frac{b_1}{\sqrt{4\,b_0 b_2 - {b_1}^2}}\right) b_1 a_1 b_2$$
$$+4\ \arctan\left(\frac{b_1}{\sqrt{4\,b_0 b_2 - {b_1}^2}}\right) a_2 b_0 b_2 - 2\ \arctan\left(\frac{b_1}{\sqrt{4\,b_0 b_2 - {b_1}^2}}\right) {b_1}^2 a_2$$

The above procedure can also be applied when the argument of the integral (5) is expanded about z = 0 in a Taylor series of order six. The resulting luminosity distance, $D_{\mathrm{L},6}$, is:

$$D_{\mathrm{L},6} = -\frac{c\,(1+z)}{\sqrt{\Omega_K} H_0} \sinh\left(\frac{\sqrt{\Omega_K} z C_T}{7680}\right) \tag{18}$$

where:

$$\begin{aligned} C_T = \quad & 315\,{\Omega_M}^5 z^5 + 350\,{\Omega_M}^4 z^5 - 420\,{\Omega_M}^4 z^4 + 400\,{\Omega_M}^3 z^5 - 480\,{\Omega_M}^3 z^4 + 480\,{\Omega_M}^2 z^5 \\ & + 600\,{\Omega_M}^3 z^3 - 576\,{\Omega_M}^2 z^4 + 640\,z^5 \Omega_M + 720\,{\Omega_M}^2 z^3 - 768\,z^4 \Omega_M + 1280\,z^5 - 960\,{\Omega_M}^2 z^2 \\ & + 960\,z^3 \Omega_M - 1536\,z^4 - 1280\,z^2 \Omega_M + 1920\,z^3 + 1920\,z \Omega_M - 2560\,z^2 + 3840\,z - 7680 \end{aligned} \tag{19}$$

The goodness of the approximation is evaluated through the percentage error, δ, which is:

$$\delta = \frac{\left|D_{\mathrm{L}}(z) - D_{\mathrm{L,app}}(z)\right|}{D_{\mathrm{L}}(z)} \times 100 \tag{20}$$

where $D_{\mathrm{L}}(z)$ is the exact luminosity distance when $\Omega_\Lambda = 0$ (see Equation (11)) and $D_{\mathrm{L,app}}(z)$ is the Taylor or Padé approximate luminosity distance; see also Formula (2.12) in [1].

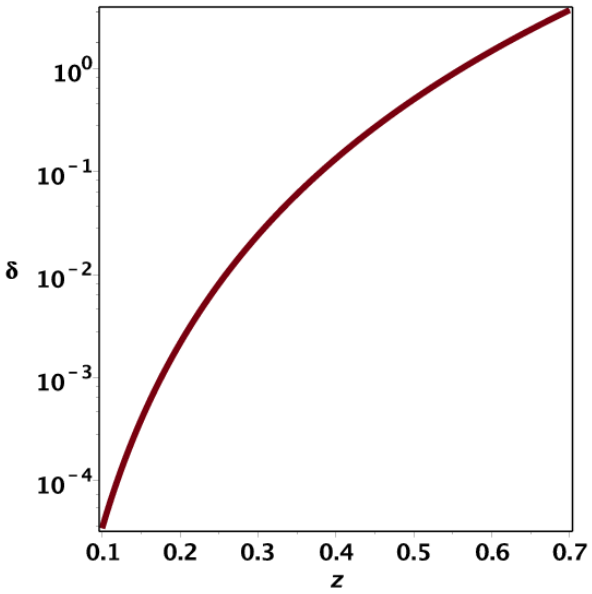

Figure 1. Percentage error, δ, relative to the Taylor approximated luminosity distance (see Equation (18)) when $H_0 = 69.6\ \mathrm{km\,s^{-1}\,Mpc^{-1}}$ and $\Omega_{\mathrm{M}} = 0.9$.

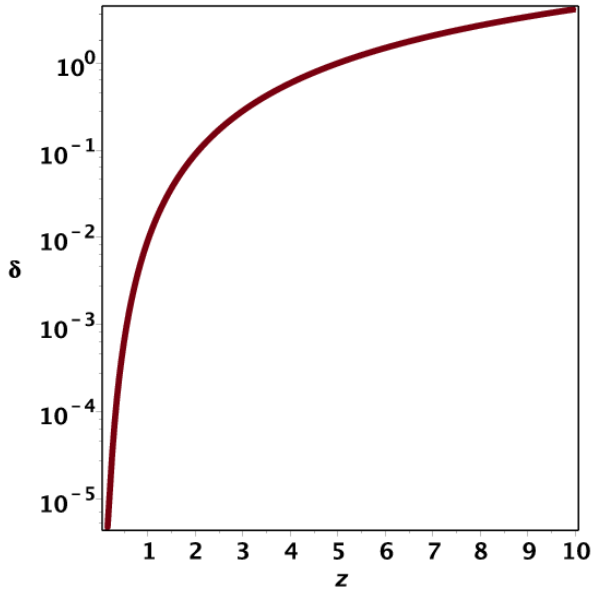

Figure 2. Percentage error, δ, relative to the Padè approximated luminosity distance (see Equation (14)) when $H_0 = 69.6\ \mathrm{km\,s^{-1}\,Mpc^{-1}}$ and $\Omega_\mathrm{M} = 0.9$.

Figures 1 and 2 report the percentage error as a function of the redshift z for the Taylor and Padé approximations, respectively. The Padé approximation is superior to the truncated Taylor expansion, because $\delta \approx 4$ is reached at $z = 10$ for the Padé approximant and at $z = 0.7$ for the Taylor expansion.

2.2. The Presence of Poles

The integrand of (5) contains poles or singularities for a given set of parameters; see Figure 3.

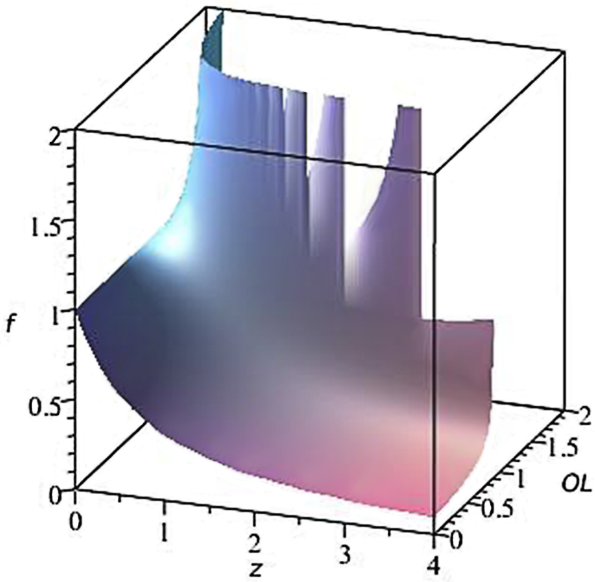

Figure 3. Behavior of $\frac{1}{E(z)}$ as a function of z and Ω_Λ in the neighborhoods of the poles when $\Omega_K = 0.11$.

The equation which models the poles is:

$$E(z) = 0 \tag{21}$$

The exact solution of the above equation $z(\Omega_\Lambda; \Omega_K = 0.11)$ is shown in Figure 4, together with the Padé approximated solution $z_{2,2}(\Omega_\Lambda; \Omega_K = 0.11)$. Is therefore possible to conclude that the Padé approximation shifts the locations of the poles by Δz; this shift expressed as a percentage error is $\delta \approx 17\%$ in the considered interval $\Omega_\Lambda = [1.15, 1.85]$.

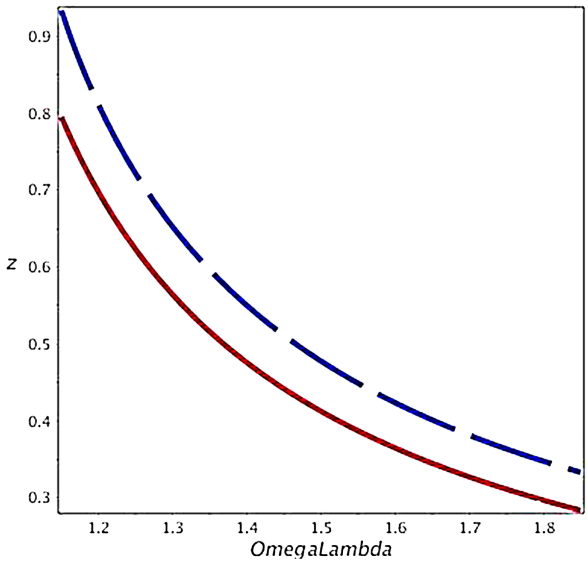

Figure 4. The exact solution for the zero in E(z), full red line, and Padé approximated solution, dashed blue line, when $\Omega_K = 0.11$.

2.3. An Astrophysical Application

We now have a Padé approximant expression for the distance modulus as a function of of H_0, Ω_M and Ω_Λ. We now perform an astronomical test on the 580 SNe in the Union 2.1 compilation (see [5]) and on the 740 SNe in the joint light-curve analysis (JLA). The JLA compilation is available at the Strasbourg Astronomical Data Center (CDS) and consists of SNe (Type I-a) for which we have a heliocentric redshift, z, apparent magnitude $m_B^\star$ in the B band, error in $m_B^\star$, $\sigma_{m_B^\star}$, parameter $X1$, error in $X1$, σ_{X1}, parameter C, error in the parameter C, σ_C and $\log_{10}(M_{stellar})$. The observed distance modulus is defined by Equation (4) in [6]:

$$m - M = -C\beta + X1\,\alpha - M_b + m_B^\star \tag{22}$$

The adopted parameters are $\alpha = 0.141$, $\beta = 3.101$ and:

$$M_b = \begin{cases} -19.05 & \text{if } M_{stellar} < 10^{10} M_\odot \\ -19.12 & \text{if } M_{stellar} \geqslant 10^{10} M_\odot \end{cases} \tag{23}$$

see Line 1 in Table 10 of [6]. The uncertainty in the observed distance modulus, σ_{m-M}, is found by implementing the error propagation equation (often called the law of errors of Gauss) when the covariant terms are neglected; see Equation (3.14) in [11],

$$\sigma_{m-M} = \sqrt{\alpha^2 {\sigma_{X1}}^2 + \beta^2 {\sigma_C}^2 + {\sigma_{m_B^\star}}^2} \tag{24}$$

The three astronomical parameters in question, H_0, Ω_M and Ω_Λ, can be derived trough the Levenberg–Marquardt method (subroutine MRQMINin [12]) once an analytical expression for the derivatives of the distance modulus with respect to the unknown parameters is provided. As a practical example, the derivative of the distance modulus, $(m-M)_{2,2}$, with respect to H_0 is:

$$\frac{d(m-M)_{2,2}}{dH_0} = -5\,\frac{1}{H_0 \ln(10)} \tag{25}$$

This numerical procedure minimizes the merit function χ^2 evaluated as:

$$\chi^2 = \sum_{i=1}^{N}\left[\frac{(m-M)_i - (m-M)(z_i)_{th}}{\sigma_i}\right]^2 \tag{26}$$

where $N = 480$, $(m-M)_i$ is the observed distance modulus evaluated at z_i, σ_i is the error in the observed distance modulus evaluated at z_i and $(m-M)(z_i)_{th}$ is the theoretical distance modulus evaluated at z_i; see Formula (15.5.5) in [12]. A reduced merit function χ^2_{red} is evaluated by:

$$\chi^2_{red} = \chi^2/NF \tag{27}$$

where $NF = n - k$ is the number of degrees of freedom, n is the number of SNe and k is the number of parameters. Another useful statistical parameter is the associated Q-value, which has to be understood as the maximum probability of obtaining a better fitting; see Formula (15.2.12) in [12]:

$$Q = 1 - GAMMQ(\frac{N-k}{2}, \frac{\chi^2}{2}) \tag{28}$$

where GAMMQ is a subroutine for the incomplete gamma function. The Akaike information criterion (AIC) (see [13]) is defined by:

$$AIC = 2k - 2ln(L) \tag{29}$$

where L is the likelihood function. We assume a Gaussian distribution for the errors, and the likelihood function can be derived from the χ^2 statistic $L \propto \exp(-\frac{\chi^2}{2})$, where χ^2 has been computed by Equation (26); see [14,15]. Now, the AIC becomes:

$$AIC = 2k + \chi^2 \tag{30}$$

Table 1 reports the three astronomical parameters for the two catalogs of SNs, and Figures 5 and 6 display the best fits.

Table 1. Numerical values of χ^2, χ^2_{red}, Q, and the AIC of the Hubble diagram for two compilations; k stands for the number of parameters. SN, supernoval; JLA, joint light-curve analysis.

Compilation	SNs	k	Parameters	$\chi 2$	χ^2_{red}	Q	AIC
Union 2.1	577	3	$H_0 = 69.81$; $\Omega_M = 0.239$; $\Omega_\Lambda = 0.651$	562.699	0.975	0.657	568.699
JLA	740	3	$H_0 = 69.398$; $\Omega_M = 0.181$; $\Omega_\Lambda = 0.538$	625.733	0.849	0.998	631.733

In order to see how $\chi 2$ varies around the minimum found by the Levenberg–Marquardt method, Figure 7 presents a 2D color map for the values of $\chi 2$ when H_0 and Ω_M are allowed to vary around the numerical values, which fix the minimum.

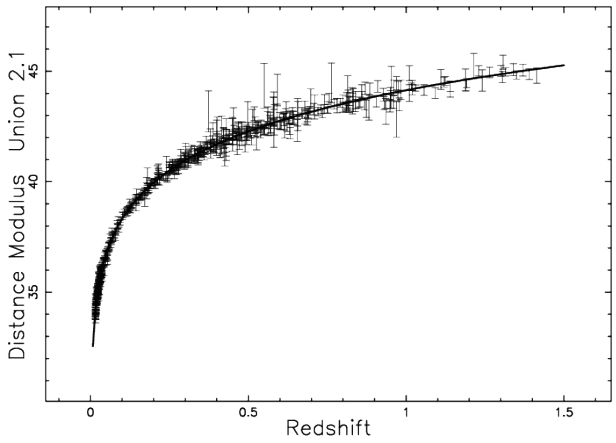

Figure 5. Hubble diagram for the Union 2.1 compilation. The solid line represents the best fit for the approximate distance modulus as represented by Equation (17); parameters as in Table 1.

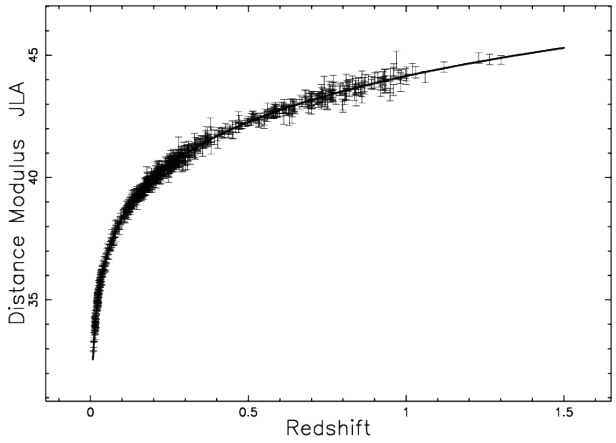

Figure 6. Hubble diagram for the JLA compilation. The solid line represents the best fit for the approximate distance modulus as given by Equation (17); parameters as in Table 1.

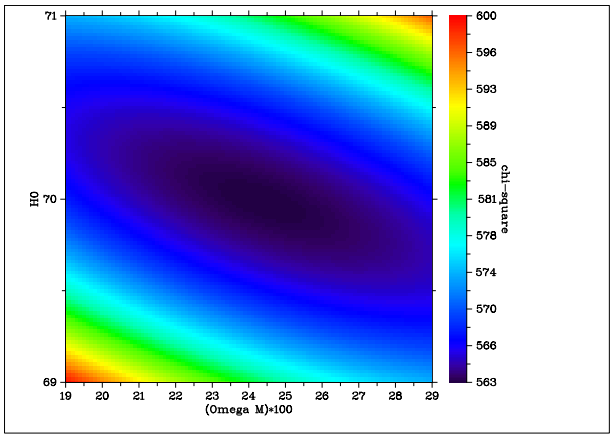

Figure 7. Color contour plot for $\chi 2$ of the Hubble diagram for the Union 2.1 compilation when H_0 and Ω_M are variables and $\Omega_\Lambda = 0.651$.

The Padé approximant distance modulus has a simple expression when the minimax rational approximation is used, as an example $p = 3, q = 2$; see Appendix C for the meaning of p and q. In the case of the Union 2.1 compilation, the approximation of Formula (17) with the parameters of Table 1 over the range in $z \in [0, 4]$ gives the following minimax equation:

$$(m - M)_{3,2} = \frac{0.359725 + 5.612031\, z + 5.627811\, z^2 + 0.054794\, z^3}{0.010587 + 0.137541\, z + 0.115904\, z^2} \quad Union\ 2.1\ compilation \tag{31}$$

the maximum error being 0.0024. The maximum error of the polynomial approximation as a function of p and q is shown in Table 2.

Table 2. The maximum error in the minimax rational approximation for the distance modulus in the case of the Union 2.1 compilation.

p	q	**Maximum Error**
1	1	0.2872
2	2	0.0197
3	2	0.0024
3	3	0.0006

In the case of the JLA compilation, the minimax equation is:

$$(m - M)_{3,2} = \frac{0.442988 + 6.355991\, z + 5.40531\, z^2 + 0.044133\, z^3}{0.012985 + 0.154698\, z + 0.109749\, z^2} \quad JLA\ compilation \tag{32}$$

the maximum error being 0.003.

The maximum difference between the two minimax formulas, which approximate the distance modulus, Equations (31) and (32), is at $z = 4$ and is 0.0584 mag. In the case of the luminosity distance as given by the Padé approximation (see Equation (14)), the minimax approximation gives:

$$D_{\mathrm{L},3,2} = \frac{-7.7618 - 1788.535\, z - 3203.0635\, z^2 - 65.8463\, z^3}{-0.438 - 0.3348\, z + 0.02039\, z^2}\, Mpc \qquad Union\ 2.1 \tag{33a}$$

$$D_{\mathrm{L},3,2} = \frac{-1.1674 - 2413.8956\, z - 2831.4248\, z^2 - 100.2959\, z^3}{-0.562 - 0.2367\, z + 0.007746\, z^2}\, Mpc \qquad JLA \tag{33b}$$

3. Application at High Redshift

This section introduces a new luminosity function (LF) for galaxies, which has a lower and an upper bound. The presence of a lower bound for the luminosity of galaxies allows one to model the evolution of the LF as a function of the redshift.

3.1. The Schechter Luminosity Function

The Schechter LF, after [16], is the standard LF for galaxies:

$$\Phi(\frac{L}{L^*})dL = (\frac{\Phi^*}{L^*})(\frac{L}{L^*})^{\alpha} \exp\left(-\frac{L}{L^*}\right)dL \tag{34}$$

Here, α sets the shape, L^* is the characteristic luminosity and Φ^* is the normalization. The distribution in absolute magnitude is:

$$\Phi(M)dM = 0.921\Phi^* 10^{0.4(\alpha+1)(M^*-M)} \exp\left(-10^{0.4(M^*-M)}\right)dM \tag{35}$$

where M^* is the characteristic magnitude.

3.2. The Gamma Luminosity Function

The *gamma* LF is:

$$f(L;\Psi^*,L^*,c)=\Psi^*\frac{\left(\frac{L}{L^*}\right)^{c-1}\mathrm{e}^{-\frac{L}{L^*}}}{L^*\Gamma(c)} \tag{36}$$

where Ψ^* is the total number of galaxies per unit Mpc^3,

$$\Gamma(z)=\int_0^\infty e^{-t}t^{z-1}dt \tag{37}$$

is the gamma function, $L^*>0$ is the scale and $c>0$ is the shape; see Formula (17.23) in [17]. Its expected value is:

$$E(\Psi^*,L^*,c)=\Psi^*L^*c \tag{38}$$

The change of parameter $(c-1)=\alpha$ allows obtaining the same scaling as for the Schechter LF (34).

3.3. The Truncated Gamma Luminosity Function

We assume that the luminosity L takes values in the interval $[L_l,L_u]$ where the indices l and u mean lower and upper; the truncated gamma LF is:

$$f(L;\Psi^*,L^*,c,L_l,L_u)=\Psi^*\,k\,(\frac{L}{L^*})^{c-1}\mathrm{e}^{-\frac{L}{L^*}} \tag{39}$$

where Ψ^* is the total number of galaxies per unit Mpc^3, and the constant k is:

$$k=\frac{c}{L^*\left(\left(\frac{L_u}{L^*}\right)^c\mathrm{e}^{-\frac{L_u}{L^*}}-\Gamma\left(1+c,\frac{L_u}{L^*}\right)+\Gamma\left(1+c,\frac{L_l}{L^*}\right)-\left(\frac{L_l}{L^*}\right)^c\mathrm{e}^{-\frac{L_l}{L^*}}\right)} \tag{40}$$

where:

$$\Gamma(a,z)=\int_z^\infty t^{a-1}e^{-t}dt \tag{41}$$

is the upper incomplete gamma function; see [18,19]. Its expected value is:

$$E(\Psi^*,L^*,c,L_l,L_u)=\Psi^*\frac{-c\left(\Gamma\left(1+c,\frac{L_u}{L^*}\right)-\Gamma\left(1+c,\frac{L_l}{L^*}\right)\right)L^*}{\left(\frac{L_u}{L^*}\right)^c\mathrm{e}^{-\frac{L_u}{L^*}}-\Gamma\left(1+c,\frac{L_u}{L^*}\right)+\Gamma\left(1+c,\frac{L_l}{L^*}\right)-\left(\frac{L_l}{L^*}\right)^c\mathrm{e}^{-\frac{L_l}{L^*}}} \tag{42}$$

More details on the truncated gamma PDF can be found in [20,21]. The four luminosities L, L_l, L^* and L_u are connected to the absolute magnitude M, M_l, M_u and M^* through the following relationship:

$$\frac{L}{L_\odot}=10^{0.4(M_\odot-M)},\frac{L_l}{L_\odot}=10^{0.4(M_\odot-M_u)},\frac{L^*}{L_\odot}=10^{0.4(M_\odot-M^*)},\frac{L_u}{L_\odot}=10^{0.4(M_\odot-M_l)} \tag{43}$$

where the indices u and l are inverted in the transformation from luminosity to absolute magnitude, and $M_\odot$ is the absolute magnitude of the Sun in the considered band. The gamma truncated LF in magnitude is:

$$\Psi(M)dM = \frac{0.4\,c\left(10^{0.4\,M^*-0.4\,M}\right)^c e^{-10^{0.4\,M^*-0.4\,M}}\Psi^*\ (\ln(2)+\ln(5))}{D} \tag{44}$$

where

$$D = e^{-10^{-0.4\,M_l+0.4\,M^*}}\left(10^{-0.4\,M_l+0.4\,M^*}\right)^c - e^{-10^{0.4\,M^*-0.4\,M_u}}\left(10^{0.4\,M^*-0.4\,M_u}\right)^c$$
$$-\Gamma\left(1+c, 10^{-0.4\,M_l+0.4\,M^*}\right)+\Gamma\left(1+c, 10^{0.4\,M^*-0.4\,M_u}\right) \tag{45}$$

The first test on the reliability of the truncated gamma LF was performed on the data of the Sloan Digital Sky Survey (SDSS) (see [22]) in the band z^*. The number of variables can be reduced to two once M_u and M_l are identified with the maximum and minimum absolute magnitude of the considered sample. The LFs considered here are displayed in Figure 8. A *second* test is represented by the behavior of the LF at high z. We expect a progressive decrease of the low luminosity galaxies (high magnitude) when z is increasing. A formula that models the previous statement can be obtained by Equation (16), which models the absolute magnitude, M, as a function of the redshift, inserting as the apparent magnitude, m, the limiting magnitude of the considered catalog. We now outline how to build an observed LF for a galaxy in a consistent way; the selected catalog is zCOSMOS, which is made up of 9697 galaxies up to z =4; see [23]. The observed LF for zCOSMOS can be built by employing the following algorithm.

(1) The minimax approximation for the luminosity distance in the case of the JLA compilation parameters (see Equation (33b)) allows fixing the distance, in the following r, once z is given.
(2) A value for the redshift is fixed, z, as well as the thickness of the layer, Δz.
(3) All of the galaxies comprised between z and Δz are selected.
(4) The absolute magnitude is computed from Equation (16).
(5) The distribution in magnitude is organized in frequencies *versus* absolute magnitude.
(6) The frequencies are divided by the volume, which is $V = \Omega\pi r^2\Delta r$, where r is the considered radius, Δr is the thickness of the radius and Ω is the solid angle of ZCOSMOS.
(7) The error in the observed LF is obtained as the square root of the frequencies divided by the volume.

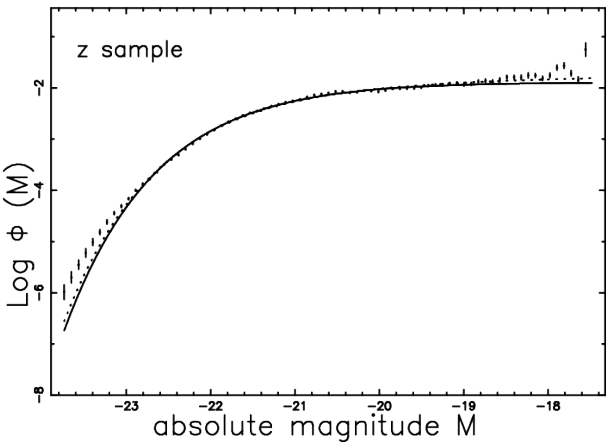

Figure 8. The luminosity function data of the Sloan Digital Sky Survey (SDSS) (z^*) are represented with error bars. The continuous line fit represents our truncated gamma luminosity function (LF) (44) with parameters $M_l = -23.73$, $M_u = -17.48$, $M^* = -21.1$, $\Psi^* = 0.04\,Mpc^{-3}$ and $c = 0.02$. The dotted line represents the Schechter LF with parameters $\Phi^* = 0.013\,Mpc^{-3}$ and $\alpha = -1.07$.

Figures 9–11 present the LF of zCOOSMOS, as well as the fit with the truncated beta LF at $z = 0.2$, $z = 0.4$ and $z = 0.6$, respectively.

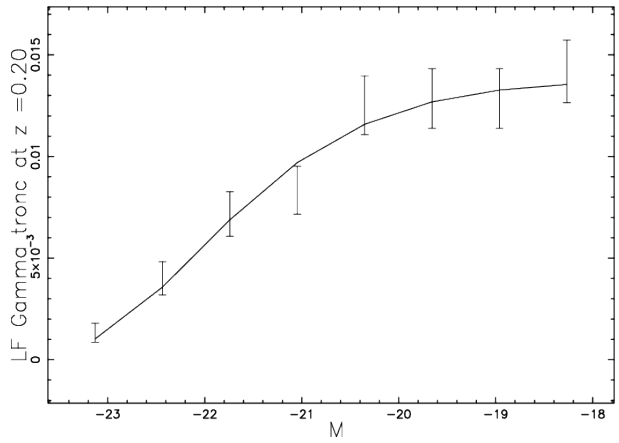

Figure 9. The luminosity function data of zCOSMOS are represented with error bars. The continuous line fit represents our gamma truncated LF (44); the chosen redshift is $z = 0.2$ and $\Delta z = 0.05$. The parameters independent of the redshift are given in Table 3, and the upper magnitude-zrelationship is given in Table 4.

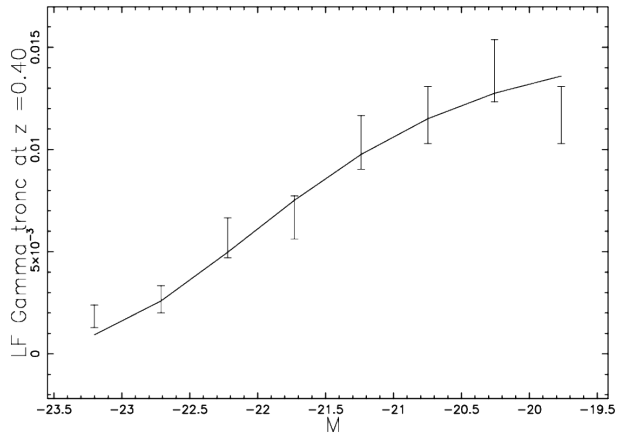

Figure 10. The luminosity function data of zCOSMOSare represented with error bars. The continuous line fit represents our gamma truncated LF (44); the chosen redshift is $z = 0.4$ and $\Delta z = 0.05$. Parameters in Tables 3 and 4.

Table 3. Parameters of the gamma truncated LF independent of z when $c = 0.01$.

$\mathbf{M}_l$	$\mathbf{M}^*$	**c**
−23.47	−22.7	0.01

Table 4. Upper magnitude, M_u (mag), and normalization, Ψ^* Mpc^{-3}, dependence on z when $c = 0.01$.

z	Ψ^*	$\mathbf{M}_u$
0.2	0.0659	−16.76
0.4	0.0459	−18.48
0.6	0.0479	−19.55

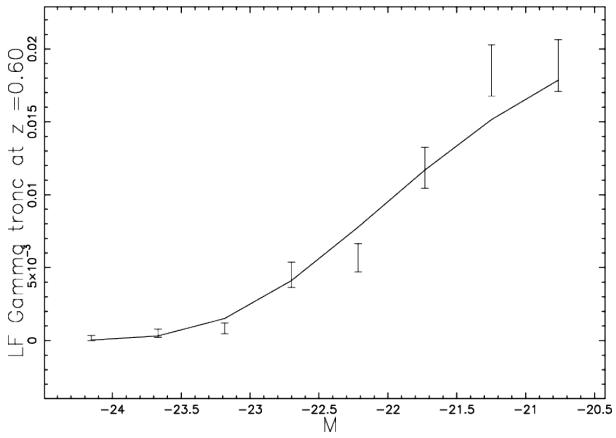

Figure 11. The luminosity function data of zCOSMOS are represented with error bars. The continuous line fit represents our gamma truncated LF (44); the chosen redshift is $z = 0.6$ and $\Delta z = 0.05$. Parameters in Tables 3 and 4.

4. Different Cosmologies

Here, we analyze the distance modulus for SNe in other cosmologies in the framework of general relativity (GR), an expanding flat universe, special relativity (SR) and a Euclidean static universe.

4.1. Simple GR Cosmology

In the framework of GR, the received flux, f, is:

$$f = \frac{L}{4\,\pi d_L^2} \tag{46}$$

where d_L is the luminosity distance, which depends on the cosmological model adopted; see Equation (7.21) in [24] or Equation (5.235) in [25].

The distance modulus in the simple GR cosmology is:

$$m - M = 43.17 - \frac{1}{\ln(10)} \ln\left(\frac{H_0}{70}\right) + 5\,\frac{\ln(z)}{\ln(10)} + 1.086\ (1 - q_0)\, z \tag{47}$$

see Equation (7.52) in [24]. The number of free parameters in the simple GR cosmology is two: H_0 and q_0.

4.2. Flat Expanding Universe

This model is based on the standard definition of luminosity in the flat expanding universe. The luminosity distance, r'_L, is:

$$r'_L = \frac{c}{H_0} z \tag{48}$$

and the distance modulus is:

$$m - M = -5\log_{10} + 5\log_{10} r'_L + 2.5\log(1 + z) \tag{49}$$

see Formulae (13) and (14) in [26]. The number of free parameters in the flat expanding model. is one: H_0.

4.3. Einstein–De Sitter Universe in SR

In the Einstein–De Sitter model, which is developed in SR, the luminosity distance, after [27,28], is:

$$d_L = 2\,\frac{c\left(1+z-\sqrt{z+1}\right)}{H_0} \tag{50}$$

and the distance modulus for the Einstein–De Sitter model is:

$$m - M = 25 + 5\,\frac{1}{\ln(10)}\ln\left(2\,\frac{c\left(1+z-\sqrt{z+1}\right)}{H_0}\right) \tag{51}$$

The number of free parameters in the Einstein–De Sitter model is one: H_0.

4.4. Milne Universe in SR

In the Milne model, which is developed in the framework of SR, the luminosity distance, after [29–31], is:

$$d_L = \frac{c\left(z+\frac{1}{2}z^2\right)}{H_0} \tag{52}$$

and the distance modulus for the Milne model is:

$$m - M = 25 + 5\,\frac{1}{\ln(10)}\ln\left(\frac{c\left(z+\frac{1}{2}z^2\right)}{H_0}\right) \tag{53}$$

The number of free parameters in the Milne model is one: H_0.

4.5. Plasma Cosmology

In a Euclidean static framework, among many possible absorption mechanisms, we selected a photo-absorption process between the photon and the electron in the IGM. This relativistic process produces a nonlinear dependence between redshift and distance:

$$z = (\exp(H_0\,d) - 1) \tag{54}$$

see Equation (4) in [32]. The previous equation is identical to our Equation (59). The Hubble constant in this first plasma model is:

$$H_0 = 1.2649\,10^8 < n_e > \ \mathrm{km\ s^{-1}\ Mpc^{-1}} \tag{55}$$

where $<n_e>$ is expressed in cgsunits. The second mechanism is a plasma effect, which produces the following relationship:

$$d = \frac{c}{H_0}\ln(1+z) \tag{56}$$

see Equation (50) in [33]. Furthermore, this second mechanism produces the same nonlinear d-z dependence as our Equation (59). In the presence of plasma absorption, the observed flux is:

$$f = \frac{L\cdot\exp\left(-bd - H_0 d - 2H_0 d\right)}{4\pi d^2} \tag{57}$$

where the factor $\exp(-bd)$ is due to Galactic and host galactic extinctions, $-H_0 d$ is reduction to the plasma in the IGM and $-2H_0 d$ is the reduction due to Compton scattering; see the formula before Equation (51) in [33]. The resulting distance modulus in the plasma mechanism is:

$$m - M = 5\,\frac{\ln\left(\ln\left(z+1\right)\right)}{\ln\left(10\right)} + \frac{15}{2}\,\frac{\ln\left(z+1\right)}{\ln\left(10\right)} + 5\,\frac{1}{\ln\left(10\right)}\ln\left(\frac{c}{H_0}\right) + 25 + 1.086\,b \tag{58}$$

see Equation (7) in [34]. The number of free parameters in the plasma cosmology is one: H_0 when $b = 0$.

4.6. Modified Tired Light

In a Euclidean static framework, the modified tired light (MTL) has been introduced in Section 2.2 in [35]. The distance in MTL is:

$$d = \frac{c}{H_0}\ln(1+z) \tag{59}$$

The distance modulus in the modified tired light (MTL) is:

$$m - M = \frac{5}{2}\,\frac{\beta\,\ln\left(z+1\right)}{\ln\left(10\right)} + 5\,\frac{1}{\ln\left(10\right)}\ln\left(\frac{\ln\left(z+1\right)c}{H_0}\right) + 25 \tag{60}$$

Here, β is a parameter comprised between one and three, which allows one to match theory with observations. The number of free parameters in MTL is two: H_0 and β.

4.7. Results for Different Cosmologies

The statistical parameters for the different cosmologies here analyzed can be found in Table 5 in the case of the Union 2.1 compilation and in Table 6 for the JLA compilation.

Table 5. Numerical values of χ^2, χ^2_{red}, Q and the AIC of the Hubble diagram for the Union 2.1 compilation; k stands for the number of parameters; H_0 is expressed in $\mathrm{km\,s^{-1}\,Mpc^{-1}}$.

Cosmology	Equation	k	Parameters	$\chi2$	χ^2_{red}	Q	AIC
simple (GR)	(47)	2	$H_0 = 73.79 \pm 0.024$, $q_0 = -0.1$	689.34	1.194	$8.6\ 10^{-4}$	793.34
flat expanding model	(49)	1	$H_0 = 66.84 \pm 0.22$	653	1.12	0.017	655
Einstein–De Sitter (SR)	(51)	1	$H_0 = 63.17 \pm 0.2$	1171.39	2.02	$2\ 10^{-42}$	1173.39
Milne (SR)	(53)	1	$H_0 = 67.53 \pm 0.22$	603.37	1.04	0.23	605.37
plasma (Euclidean)	(58)	1	$H_0 = 74.2 \pm 0.24$	895.53	1.546	$5.2\ 10^{-16}$	897.5
MTL (Euclidean)	(60)	2	$\beta = 2.37$, $H_0 = 69.32 \pm 0.34$	567.96	0.982	0.609	571.9

Table 6. Numerical values of χ^2, χ^2_{red}, Q and the AIC of the Hubble diagram for the JLA compilation; k stands for the number of parameters; H_0 is expressed in $\mathrm{km\,s^{-1}\,Mpc^{-1}}$.

Cosmology	Equation	k	Parameters	$\chi2$	χ^2_{red}	Q	AIC
simple (GR)	(47)	2	$H_0 = 73.79 \pm 0.023$, $q_0 = -0.14$	749.14	1.016	0.369	755.14
flat expanding model	(49)	1	$H_0 = 66.49 \pm 0.18$	717.3	0.97	0.709	719.3
Einstein–De Sitter (SR)	(51)	1	$H_0 = 62.57 \pm 0.17$	1307.75	1.76	$3.27\ 10^{-34}$	1309.75
Milne (SR)	(53)	1	$H_0 = 67.19 \pm 0.18$	656.11	0.887	0.986	658.11
plasma (Euclidean)	(58)	1	$H_0 = 74.45 \pm 0.2$	1017.79	1.377	$3.59\ 10^{-11}$	1019.79
MTL (Euclidean)	(60)	2	$\beta = 2.36$, $H_0 = 69.096 \pm 0.32$	626.27	0.848	0.998	630.27

5. Conclusions

5.1. Padé approximant

It is generally thought that in the case of the luminosity distance, the Padé approximant is more accurate than the Taylor expansion. As an example, at $z = 1.5$, which is the maximum value of the redshift here considered, the percentage error of the luminosity distance is $\delta = 0.036\%$ in the case of the Padé approximation. In the case of of the Taylor expansion, $\delta = 0.036\%$ for the luminosity distance is

reached $z = 0.322$, which means a more limited range of convergence than for the Padé approximation. Once a precise approximation for the luminosity distance was obtained (see Equation (11)), we derived an approximate expression for the distance modulus (see Equation (17)) and the absolute magnitude (see Equation (16)).

5.2. Astrophysical Applications

The availability of the observed distance modulus for a great number of SNs of Type Ia allows deducing H_0, Ω_M and Ω_Λ for two catalogs; see Table 1. In order to derive the above parameters, the Levenberg–Marquardt method was implemented, and therefore, the first derivative of the distance modulus (see Equation (17)) with respect to three parameters is provided. The value of H_0 is a matter of research rather than a well-defined constant. As an example, a recent evaluation with a sample of Cepheids gives $H_0 = 73.8\ \mathrm{km\,s^{-1}\,Mpc^{-1}}$; see [36]. Once the above value is considered the 'true' value, we have found, adopting the Padé approximant, $H_0 = 69.81\ \mathrm{km\,s^{-1}\,Mpc^{-1}}$, which means a percentage error $\delta = 5.4\%$, for the Union 2.1 compilation, and $H_0 = 69.398\ \mathrm{km\,s^{-1}\,Mpc^{-1}}$, which means a percentage error $\delta = 5.9\%$, for the JLA compilation; see Table 1.

5.3. Evolutionary Effects

The evolution of the LF for galaxies as a function of the redshift is here modeled by an upper and lower truncated gamma PDF. This choice allows modeling the lower bound in luminosity (the higher bound in absolute magnitude) according to the evolution of the absolute magnitude; see Equation (16). According to the LF here considered (see Equation (44)), the evolution with z of the LF is simply connected to the evolution of the higher bound in absolute magnitude; see Figures 9–11. Is not necessary to modify the shape parameters of the LF, which are c and M^*, but only to calculate the normalization Ψ^* at different values of the redshift.

5.4. Statistical Tests for Union 2.1

In the case of the Union 2.1 compilation, the best results for χ^2_{red} are obtained by the ΛCDM cosmology (GR), $\chi^2_{red} = 0.975$, against $\chi^2_{red} = 0.982$ of the MTL cosmology (Euclidean), but the situation is inverted when the AIC is considered: the AIC is 571.9 for the MTL cosmology and 568.7 for the ΛCDM cosmology (GR); see Tables 1 and 5.

The simple model (GR), the Einstein–De Sitter model (SR), the Milne model (SR) and the plasma model (Euclidean) are rejected because the reduced merit function χ^2_{red} is smaller than one; see Table 5. The best performing one-parameter model is that of Milne, $\chi^2_{red} = 1.04$, followed by the flat expanding model, $\chi^2_{red} = 1.12$; see Table 5.

5.5. Statistical Tests for JLA

In the case of the JLA compilation, the best results for χ^2_{red} are obtained by the MTL cosmology (Euclidean), $\chi^2_{red} = 0.848$, against $\chi^2_{red} = 0.849$ for the ΛCDM cosmology (GR); see Tables 1 and 6. The simple model (GR), the Einstein–De Sitter model (SR) and the plasma model (Euclidean) are rejected because the reduced merit function χ^2_{red} is smaller than one; see Table 6. In the case of the JLA, the test on the Milne model is positive because χ^2_{red} is smaller than one. The best performing one-parameter model is that of Milne, $\chi^2_{red} = 0.887$, followed by the flat expanding model, $\chi^2_{red} = 0.97$; see Table 6.

5.6. Different Approaches

Table 7 reports six items connected to the use of the Padé approximant in Cosmology: the letters Y/N indicate if the item is treated or not, and the columns identifies the paper in question; LF means the luminosity function for galaxies.

Table 7. Arguments treated in papers on Padé approximants and here.

Problem	Aviles 2014	Wei 2014	Adachi 2012	Here
luminosity distance	*Y*	*Y*	*Y*	*Y*
distance modulus	*Y*	*Y*	*Y*	*Y*
empty beam	*N*	*N*	*Y*	*N*
distance modulus minimax	*N*	*N*	*N*	*Y*
poles	*N*	*N*	*N*	*Y*
LF=f(z)	*N*	*N*	*N*	*Y*

Conflicts of Interest: The authors declare no conflict of interest.

Appendix

A. The Padé Approximant

Given a function $f(z)$, the Padé approximant, after [37], is:

$$f(z) = \frac{a_0 + a_1 z + \cdots + a_p z^p}{b_0 + b_1 z + \cdots + b_q z^q} \tag{A1}$$

where the notation is the same as in [19].

The coefficients a_i and b_i are found through Wynn's cross rule (see [38,39]), and our choice is $p = 2$ and $q = 2$. The choice of p and q is a compromise between precision, high values for p and q and the simplicity of the expressions to manage low values for p and q; Appendix B gives three different approximations for the indefinite integral for three different combinations in p and q. In the case in which $b_0 \neq 0$, we can divide both the numerator and denominator by b_0, reducing by one the number of parameters; see as an example [40].

The integrand of Equation (5) is:

$$\frac{1}{E(z)} = \frac{1}{\sqrt{\Omega_{\mathrm{M}}\,(1+z)^3 + \Omega_K\,(1+z)^2 + \Omega_\Lambda}} \tag{A2}$$

and the Padé approximant gives:

$$\frac{1}{E(z)} = \frac{a_0 + a_1 z + a_2 z^2}{b_0 + b_1 z + b_2 z^2} \tag{A3}$$

where:

$$\begin{aligned} a_0 = \quad & 16\,(32\,{\Omega_K}^3\Omega_\Lambda + 16\,{\Omega_K}^2{\Omega_\Lambda}^2 + 160\,{\Omega_K}^2\Omega_\Lambda\,\Omega_M + 24\,{\Omega_K}^2{\Omega_M}^2 + 64\,\Omega_K\,{\Omega_\Lambda}^2\Omega_M \\ & + 320\,\Omega_K\,\Omega_\Lambda\,{\Omega_M}^2 + 40\,\Omega_K\,{\Omega_M}^3 + 96\,{\Omega_\Lambda}^2{\Omega_M}^2 \\ & + 192\,\Omega_\Lambda\,{\Omega_M}^3 + 15\,{\Omega_M}^4)\,(\Omega_M + \Omega_K + \Omega_\Lambda)^4 \end{aligned} \tag{A4}$$

$$\begin{aligned} a_1 = \quad & 4\,(128\,{\Omega_K}^4\Omega_\Lambda + 32\,{\Omega_K}^3{\Omega_\Lambda}^2 + 704\,{\Omega_K}^3\Omega_\Lambda\,\Omega_M - 16\,{\Omega_K}^2{\Omega_\Lambda}^2\Omega_M \\ & + 1456\,{\Omega_K}^2\Omega_\Lambda\,{\Omega_M}^2 + 32\,{\Omega_K}^2{\Omega_M}^3 - 64\,\Omega_K\,{\Omega_\Lambda}^3\Omega_M - 384\,\Omega_K\,{\Omega_\Lambda}^2{\Omega_M}^2 \\ & + 1512\,\Omega_K\,\Omega_\Lambda\,{\Omega_M}^3 + 50\,\Omega_K\,{\Omega_M}^4 - 192\,{\Omega_\Lambda}^3{\Omega_M}^2 - 288\,{\Omega_\Lambda}^2{\Omega_M}^3 + 648\,\Omega_\Lambda\,{\Omega_M}^4 \\ & + 15\,{\Omega_M}^5)\,(\Omega_M + \Omega_K + \Omega_\Lambda)^3 \end{aligned} \tag{A5}$$

$$
\begin{aligned}
a_2 = \quad & -\left(256\,{\Omega_K}^4\Omega_\Lambda\,\Omega_M - 64\,{\Omega_K}^3{\Omega_\Lambda}^3 + 320\,{\Omega_K}^3{\Omega_\Lambda}^2\Omega_M + 960\,{\Omega_K}^3\Omega_\Lambda\,{\Omega_M}^2\right.\\
& -320\,{\Omega_K}^2{\Omega_\Lambda}^3\Omega_M + 240\,{\Omega_K}^2{\Omega_\Lambda}^2{\Omega_M}^2 + 1440\,{\Omega_K}^2\Omega_\Lambda\,{\Omega_M}^3 + 16\,{\Omega_K}^2{\Omega_M}^4\\
& -1600\,\Omega_K\,{\Omega_\Lambda}^3{\Omega_M}^2 - 480\,\Omega_K\,{\Omega_\Lambda}^2{\Omega_M}^3 + 1140\,\Omega_K\,\Omega_\Lambda\,{\Omega_M}^4 + 20\,\Omega_K\,{\Omega_M}^5\\
& -256\,{\Omega_\Lambda}^4{\Omega_M}^2 - 1600\,{\Omega_\Lambda}^3{\Omega_M}^3 - 240\,{\Omega_\Lambda}^2{\Omega_M}^4 + 380\,\Omega_\Lambda\,{\Omega_M}^5\\
& \left.+5\,{\Omega_M}^6\right)\left(\Omega_M + \Omega_K + \Omega_\Lambda\right)^2
\end{aligned} \tag{A6}
$$

$$
\begin{aligned}
b_0 = \quad & 16\left(\Omega_M + \Omega_K + \Omega_\Lambda\right)^{9/2}\left(32\,{\Omega_K}^3\Omega_\Lambda + 16\,{\Omega_K}^2{\Omega_\Lambda}^2 + 160\,{\Omega_K}^2\Omega_\Lambda\,\Omega_M\right.\\
& +24\,{\Omega_K}^2{\Omega_M}^2 + 64\,\Omega_K\,{\Omega_\Lambda}^2\Omega_M + 320\,\Omega_K\,\Omega_\Lambda\,{\Omega_M}^2 + 40\,\Omega_K\,{\Omega_M}^3\\
& \left.+96\,{\Omega_\Lambda}^2{\Omega_M}^2 + 192\,\Omega_\Lambda\,{\Omega_M}^3 + 15\,{\Omega_M}^4\right)
\end{aligned} \tag{A7}
$$

$$
\begin{aligned}
b_1 = \quad & 4\left(\Omega_M + \Omega_K + \Omega_\Lambda\right)^{7/2}\left(256\,{\Omega_K}^4\Omega_\Lambda + 96\,{\Omega_K}^3{\Omega_\Lambda}^2 + 1536\,{\Omega_K}^3\Omega_\Lambda\,\Omega_M\right.\\
& +96\,{\Omega_K}^3{\Omega_M}^2 + 336\,{\Omega_K}^2{\Omega_\Lambda}^2\Omega_M + 3696\,{\Omega_K}^2\Omega_\Lambda\,{\Omega_M}^2\\
& +336\,{\Omega_K}^2{\Omega_M}^3 - 64\,\Omega_K\,{\Omega_\Lambda}^3\Omega_M + 384\,\Omega_K\,{\Omega_\Lambda}^2{\Omega_M}^2 + 4200\,\Omega_K\,\Omega_\Lambda\,{\Omega_M}^3\\
& \left.+350\,\Omega_K\,{\Omega_M}^4 - 192\,{\Omega_\Lambda}^3{\Omega_M}^2 + 288\,{\Omega_\Lambda}^2{\Omega_M}^3 + 1800\,\Omega_\Lambda\,{\Omega_M}^4 + 105\,{\Omega_M}^5\right)
\end{aligned} \tag{A8}
$$

$$
\begin{aligned}
b_2 = \quad & \left(\Omega_M + \Omega_K + \Omega_\Lambda\right)^{5/2}\left(512\,{\Omega_K}^5\Omega_\Lambda + 384\,{\Omega_K}^4{\Omega_\Lambda}^2 + 3584\,{\Omega_K}^4\Omega_\Lambda\,\Omega_M\right.\\
& +192\,{\Omega_K}^3{\Omega_\Lambda}^3 + 1984\,{\Omega_K}^3{\Omega_\Lambda}^2\Omega_M + 10752\,{\Omega_K}^3\Omega_\Lambda\,{\Omega_M}^2 + 320\,{\Omega_K}^3{\Omega_M}^3\\
& +960\,{\Omega_K}^2{\Omega_\Lambda}^3\Omega_M + 5136\,{\Omega_K}^2{\Omega_\Lambda}^2{\Omega_M}^2 + 17760\,{\Omega_K}^2\Omega_\Lambda\,{\Omega_M}^3 + 840\,{\Omega_K}^2{\Omega_M}^4\\
& +2752\,\Omega_K\,{\Omega_\Lambda}^3{\Omega_M}^2 + 7392\,\Omega_K\,{\Omega_\Lambda}^2{\Omega_M}^3 + 15060\,\Omega_K\,\Omega_\Lambda\,{\Omega_M}^4 + 700\,\Omega_K\,{\Omega_\Lambda}^5\\
& \left.+256\,{\Omega_\Lambda}^4{\Omega_M}^2 + 2752\,{\Omega_\Lambda}^3{\Omega_M}^3 + 3696\,{\Omega_\Lambda}^2{\Omega_M}^4 + 5020\,\Omega_\Lambda\,{\Omega_M}^5 + 175\,{\Omega_M}^6\right)
\end{aligned} \tag{A9}
$$

B. The Integrals as Functions of p and q

We now present the indefinite integral of (5) for different values of p and q.
In the case $p = 1, q = 1$,

$$
F_{1,1}(z; a_0, a_1, b_0, b_1) = \frac{a_1 z}{b_1} + \frac{\ln\left(z b_1 + b_0\right) a_0}{b_1} - \frac{\ln\left(z b_1 + b_0\right) b_0 a_1}{{b_1}^2} \tag{B1}
$$

In the case $p = 2, q = 1$,

$$
\begin{aligned}
F_{2,1}(z; a_0, a_1, a_2, b_0, b_1) = 1/2\,\frac{a_2 z^2}{b_1} + \frac{a_1 z}{b_1} - \frac{z b_0 a_2}{{b_1}^2} + \frac{\ln\left(z b_1 + b_0\right) a_0}{b_1}\\
- \frac{\ln\left(z b_1 + b_0\right) b_0 a_1}{{b_1}^2} + \frac{\ln\left(z b_1 + b_0\right) a_2 {b_0}^2}{{b_1}^3}
\end{aligned} \tag{B2}
$$

In the case $p = 2, q = 2$,

$$
\begin{aligned}
& F_{2,2}(z; a_0, a_1, a_2, b_0, b_1, b_2) = \frac{a_2 z}{b_2}\\
& + \frac{1}{2}\,\frac{\ln\left(z^2 b_2 + z b_1 + b_0\right) a_1}{b_2} - \frac{1}{2}\,\frac{\ln\left(z^2 b_2 + z b_1 + b_0\right) a_2 b_1}{{b_2}^2}\\
& + 2\,\frac{a_0}{\sqrt{4\,b_0 b_2 - {b_1}^2}}\arctan\left(\frac{2\,z b_2 + b_1}{\sqrt{4\,b_0 b_2 - {b_1}^2}}\right) - 2\,\frac{a_2 b_0}{b_2\sqrt{4\,b_0 b_2 - {b_1}^2}}\arctan\left(\frac{2\,z b_2 + b_1}{\sqrt{4\,b_0 b_2 - {b_1}^2}}\right)\\
& - \frac{b_1 a_1}{b_2\sqrt{4\,b_0 b_2 - {b_1}^2}}\arctan\left(\frac{2\,z b_2 + b_1}{\sqrt{4\,b_0 b_2 - {b_1}^2}}\right) + \frac{{b_1}^2 a_2}{{b_2}^2\sqrt{4\,b_0 b_2 - {b_1}^2}}\arctan\left(\frac{2\,z b_2 + b_1}{\sqrt{4\,b_0 b_2 - {b_1}^2}}\right)
\end{aligned} \tag{B3}
$$

C. Minimax Approximation

Let $f(x)$ be a real function defined in the interval $[a, b]$. The best rational approximation of degree (k, l) evaluates the coefficients of the ratio of two polynomials of degree k and l, respectively, which minimizes the maximum difference of:

$$max\left|f(x) - \frac{p_0 + p_1 x + \cdots + p_k x^k}{q_0 + q_1 x + \cdots + q_\ell x^\ell}\right| \tag{C1}$$

on the interval $[a, b]$. The quality of the fit is given by the maximum error over the considered range. The coefficients are evaluated through the Remez algorithm; see [41,42]. As an example, the minimax of degree (2,2) of:

$$f(x) = \frac{\log(1+x)}{x} \tag{C2}$$

is:

$$f(x) = \frac{0.206888 + 0.093657\,x + 0.001573\,x^2}{0.206895 + 0.196889\,x + 0.0320939\,x^2} \tag{C3}$$

and the maximum error is $3.345\,10^{-5}$. As an example, the minimax rational function approximation is applied to the evaluation of the complete elliptic integral of the first and second kind; see [43].

References

1. Adachi, M.; Kasai, M. An Analytical Approximation of the Luminosity Distance in Flat Cosmologies with a Cosmological Constant. *Prog. Theor. Phys.* **2012**, *127*, 145–152.
2. Aviles, A.; Bravetti, A.; Capozziello, S.; Luongo, O. Precision cosmology with Padé rational approximations: Theoretical predictions versus observational limits. *Phys. Rev. D* **2014**, *90*, 043531.
3. Wei, H.; Yan, X.P.; Zhou, Y.N. Cosmological applications of Pade approximant. *J. Cosmol. Astropart. Phys.* **2014**, *1*, 45.
4. Riess, A.G.; Filippenko, A.V.; Challis, P.; Clocchiatti, A. Observational Evidence from Supernovae for an Accelerating Universe and a Cosmological Constant. *Astron. J.* **1998**, *116*, 1009–1038.
5. Suzuki, N.; Rubin, D.; Lidman, C.; Aldering, G.; Amanullah, R.; Barbary, K.; Barrientos, L.F. The Hubble Space Telescope Cluster Supernova Survey. V. Improving the Dark-energy Constraints above z greater than 1 and Building an Early-type-hosted Supernova Sample. *Astrophys. J.* **2012**, *746*, 85.
6. Betoule, M.; Kessler, R.; Guy, J.; Mosher, J. Improved cosmological constraints from a joint analysis of the SDSS-II and SNLS supernova samples. *Cosmol. Nongalactic Astrophys.* **2014**, *568*, A22.
7. Montiel, A.; Lazkoz, R.; Sendra, I.; Escamilla-Rivera, C.; Salzano, V. Nonparametric reconstruction of the cosmic expansion with local regression smoothing and simulation extrapolation. *Phys. Rev. D* **2014**, *89*, 043007.
8. Yahya, S.; Seikel, M.; Clarkson, C.; Maartens, R.; Smith, M. Null tests of the cosmological constant using supernovae. *Phys. Rev. D* **2014**, *89*, 023503.
9. Hogg, D.W. Distance measures in cosmology. **1999**, arXiv:astro-ph/9905116.
10. Peebles, P.J.E. *Principles of Physical Cosmology*; Princeton University Press: Princeton, NJ, USA, 1993.
11. Bevington, P.R.; Robinson, D.K. *Data Reduction and Error Analysis for the Physical Sciences*; McGraw-Hill: New York, NY, USA, 2003.
12. Press, W.H.; Teukolsky, S.A.; Vetterling, W.T.; Flannery, B.P. *Numerical Recipes in FORTRAN. The Art of Scientific Computing*; Cambridge University Press: Cambridge, UK, 1992.
13. Akaike, H. A new look at the statistical model identification. *IEEE Trans. Automatic Control* **1974**, *19*, 716–723.
14. Liddle, A.R. How many cosmological parameters? *Mon. Not. R. Astron. Soc.* **2004**, *351*, L49–L53.
15. Godlowski, W.; Szydowski, M. Constraints on Dark Energy Models from Supernovae. In *1604–2004: Supernovae as Cosmological Lighthouses*; Turatto, M., Benetti, S., Zampieri, L., Shea, W., Eds.; Astronomical Society of the Pacific: Orem, UT, USA, 2005; Volume 342, pp. 508–516.
16. Schechter, P. An analytic expression for the luminosity function for galaxies. *Astrophys. J.* **1976**, *203*, 297–306.

17. Johnson, N.L.; Kotz, S.; Balakrishnan, N. *Continuous Univariate Distributions*, 2nd ed.; Wiley: New York, NY, USA, 1994; Volume 1.
18. Abramowitz, M.; Stegun, I.A. *Handbook of Mathematical Functions with Formulas, Graphs, and Mathematical Tables*; Dover: New York, NY, USA, 1965.
19. Olver, F.W.J.; Lozier, D.W.; Boisvert, R.F.; Clark, C.W., Eds. *NIST Handbook of Mathematical Functions*; Cambridge University Press: Cambridge, UK, 2010.
20. Zaninetti, L. A right and left truncated gamma distribution with application to the stars. *Adv. Stud. Theor. Phys.* **2013**, *23*, 1139–1147.
21. Okasha, M.K.; Alqanoo, I.M. Inference on The Doubly Truncated Gamma Distribution For Lifetime Data. *Int. J. Math. Stat. Invent.* **2014**, *2*, 1–17.
22. Blanton, M.R.; Hogg, D.W.; Bahcall, N.A.; Brinkmann, J.; Britton, M. The Galaxy Luminosity Function and Luminosity Density at Redshift z = 0.1. *Astrophys. J.* **2003**, *592*, 819–838.
23. Lilly, S.J.; Le Brun, V.; Maier, C.; Mainieri, V. The zCOSMOS 10k-Bright Spectroscopic Sample. *Astrophys. J. Suppl.* **2009**, *184*, 218–229.
24. Ryden, B. *Introduction to Cosmology*; Addison Wesley: San Francisco, CA, USA, 2003.
25. Lang, K. *Astrophysical Formulae: Space, Time, Matter and Cosmology*; Astronomy and Astrophysics Library, Springer: Berlin, Germany, 2013.
26. Heymann, Y. On the Luminosity Distance and the Hubble Constant. *Prog. Phys.* **2013**, *3*, 5–6.
27. Einstein, A.; de Sitter, W. On the Relation between the Expansion and the Mean Density of the Universe. *Proc. Natl. Acad. Sci. USA* **1932**, *18*, 213–214.
28. Krisciunas, K. Look-Back Time the Age of the Universe and the Case for a Positive Cosmological Constant. *J. Roy. Astron. Soc. Can.* **1993**, *87*, 223.
29. Milne, E.A. World-Structure and the Expansion of the Universe. *Zeitschrift fur Astrophysik* **1933**, *6*, 1.
30. Chodorowski, M.J. Cosmology Under Milne's Shadow. *Publ. Astron. Soc. Austral.* **2005**, *22*, 287–291.
31. Adamek, J.; Di Dio, E.; Durrer, R.; Kunz, M. Distance-redshift relation in plane symmetric universes. *Phys. Rev. D* **2014**, *89*, 063543.
32. Ashmore, L. Recoil Between Photons and Electrons Leading to the Hubble Constant and CMB. *Galilean Electrodyn.* **2006**, *17*, 53.
33. Brynjolfsson, A. Redshift of photons penetrating a hot plasma. **2004**, arXiv:astro-ph/0401420.
34. Brynjolfsson, A. Magnitude-Redshift Relation for SNe Ia, Time Dilation, and Plasma Redshift. **2006**, arXiv:astro-ph/0602500.
35. Zaninetti, L. On the Number of Galaxies at High Redshift. *Galaxies* **2015**, *3*, 129–155.
36. Riess, A.G.; Macri, L.; Casertano, S.; Lampeitl, H.; Ferguson, H.C.; Filippenko, A.V.; Jha, S.W.; Li, W.; Chornock, R. A 3% Solution: Determination of the Hubble Constant with the Hubble Space Telescope and Wide Field Camera 3. *Astrophys. J.* **2011**, *730*, 119.
37. Padé, H. Sur la représentation approchée d'une fonction par des fractions rationnelles. *Ann. Sci. Ecole Norm. Sup.* **1892**, *9*, 193.
38. Baker, G. *Essentials of Padé Approximants*; Academic Press: New York, NY, USA, 1975.
39. Baker, G.A.; Graves-Morris, P.R. *Padé approximants*; Cambridge University Press: Cambridge, UK, 1996.
40. Yamada, H.S.; Ikeda, K.S. A Numerical Test of Pade Approximation for Some Functions with singularity. *Int. J. Comput. Math.* **2014**, *2014*.
41. Remez, E. Sur la détermination des polynômes d´ approximation de degré donnée. *Comm. Soc. Math. Kharkov* **1934**, *10*, 41–63.
42. Remez, E. *General Computation Methods of Chebyshev Approximation. The Problems with Linear Real Parameters*; Publishing House of the Academy of Science of the Ukrainian SSR: Kiev, Ukraine, 1957.
43. Fukushima, T. Precise and fast computation of the general complete elliptic integral of the second kind. *Math. Comput.* **2011**, *80*, 1725–1743.